energies

MDPI

Article

Evaluation of the State of Charge of a Solid/Liquid Phase Change Material in a Thermal Energy Storage Tank

Gabriel Zsembinszki [1], Christian Orozco [1], Jaume Gasia [1], Tilman Barz [2], Johann Emhofer [2] and Luisa F. Cabeza [1,*]

[1] GREiA Research Group, Universitat de Lleida, 25001 Lleida, Spain; gabriel.zsembinszki@udl.cat (G.Z.); chris.orozco.lara@gmail.com (C.O.); jaume.gasia@diei.udl.cat (J.G.)

[2] Center for Energy, AIT, Austrian Institute of Technology, 1210 Wien, Austria; Tilman.Barz@ait.ac.at (T.B.); Johann.Emhofer@ait.ac.at (J.E.)

* Correspondence: lcabeza@diei.udl.cat; Tel.: +34-973-003576

Received: 12 February 2020; Accepted: 12 March 2020; Published: 18 March 2020

Abstract: Monitoring of the state of charge of the thermal energy storage component in solar thermal systems for space heating and/or cooling in residential buildings is a key element from the overall system control strategy point of view. According to the literature, there is not a unique method for determining the state of charge of a thermal energy storage system that could generally be applied in any system. This contribution firstly provides a classification of the state-of-the-art of available techniques for the determination of the state of charge, and secondly, it presents an experimental analysis of different methods based on established sensor technologies, namely temperature, mass flow rates, and pressure measurements, tested using a lab-scale heat exchanger filled with a commercial phase change material for cooling applications. The results indicate that, depending on the expected accuracy and available instrumentation, each of the methods studied here can be used in the present application, the deviations between the methods generally being below 20%. This study concludes that a proper combination of two or more of these methods would be the ideal strategy to obtain a more reliable and accurate estimation of the state of charge of the latent heat thermal energy storage.

Keywords: phase change material; thermal energy storage; state of charge; cooling applications; residential buildings; experimental testing

1. Introduction

Worldwide energy requirements needed to sustain the continuously increasing human population, while the main source of energy, that nowadays relies on the use of fossil fuels, is limited and not enough to sustain the current trends. Furthermore, the main drawback of an excessive use of fossil fuels is the high emission of pollutants to the environment, such as CO_2, contributing to global warming. As a consequence, worldwide bodies decided to adopt policies and targets to diminish the CO_2 emissions that reached a historic level of 32.5 gigatons in 2017 [1]. Therefore, new technologies based on the use of renewable energies were developed or are still developing with the aim to reduce the use of fossil fuels and the consequent amount of CO_2 emissions. Most of these new technologies require the use of energy storage systems to reduce the mismatch between supply and demand, and to fill the gap that conventional energy sources do not have, because they can usually meet the immediate energy demand.

Improving building energy efficiency is a key element to reduce energy consumption and to maximize the use of renewable energy sources. Heat demand in residential buildings accounts for 60% to 80% of the overall energy consumption in cold climate regions, while cooling demand

accounts for 30% to 40% in warm climate regions [2]. This means that the implementation of solar thermal systems for space heating and/or cooling could be a great opportunity to substantially reduce the energy use in residential buildings. However, the main challenges related to the implementation of solar thermal systems in residential buildings are their current high installation costs with respect to conventional systems and a complex process of integration into existing housing. In addition, the effective integration of thermal energy storage (TES) systems, with their inherent dynamic operation, require a proper monitoring and advanced control strategies to realize effective operation strategies for dynamic heat integration [3,4].

For water/ice storage systems, a method based on the use of electrical conductivity sensors was applied [5–7]. The thickness of the growing ice layer on the heat exchanger surface can be seen by the different electrical conductivity between ice and water. This mature measurement technique can give accurate results for the determination of the position of a solid/liquid interface (monitoring the phase front propagation) in simple storage tank geometries applying a series of sensors in one-dimension (1D). For other types of phase change materials (PCM), or higher temperatures, no commercial solutions/measurement techniques are known to determine the State of Charge (SoC) [5] based on the electrical conductivity method. According to Paberit and Ojerborn [8], electrical measurement techniques could also be used commercially. These authors investigated the electrical resistance technique to satisfactorily determine the SoC in applications that use polymers as PCM.

Methods based on the use of pressure sensors to detect changes in the volume of the PCM can also be used to determine the phase fraction of the storage material, thus the SoC of a PCM tank. This technique was investigated by, for example, Steinmaurer et al. [9] and Paberit and Ojerborn [8], but no results were presented. Bissell and Gataora [10] proposed a concept based on a pressure measurement in the storage tank and the transformation of measured pressures into state of charge via a look-up table.

One of the most studied methods used for monitoring of storage tanks is by means of temperature sensors located in (or near) the PCM. Together with the knowledge of the specific melting point of the PCM, this information allows a statement on the condition of the PCM, being either solid or liquid, and therefore, on the SoC. In Grama et al. [11], a thermal energy battery with enhanced heat exchange capability and modularity was developed, in which the temperature in the heat transfer fluid at the bottom of a simple storage tank filled with PCM was monitored. Dixler and Kwok [12] used two temperature sensors (central and at the edge of the PCM) to determine the state of the PCM in an electrical energy storage with storage cells embedded in a PCM. Ros [13] measured the temperature distribution in the PCM enveloping a thermally insulated container by means of several temperature sensors to determine the insulation time. Viessmann Kaeltetechnik [14] determined the SoC of a thermal energy storage composed of an arbitrary number of cells with storage media for a cooling chamber or room. Each medium can have different phase change temperatures, and a temperature measuring device is arranged in the individual storage cells to detect the temperature of the storage medium in the respective storage cell and transmits it to a device that calculates the SoC based on the known actual temperatures and known phase change temperatures. Kazuhiro et al. [15] used a similar device as Viessmann Kaeltetechnik [14] for the application of a storage chamber equipped with latent heat storage materials. The main limitation of the aforementioned methods is the application of point (local) measurements, which give accurate results only for homogeneous temperature fields in the PCM, storage tank, and storage internals. For inhomogeneous temperatures, these point measurements can only realize a poor resolution of temperature fields and the position of phase fronts.

To improve the accuracy of the estimation of the solid/liquid phase fraction of the PCM, Barz [16] developed a method based on the determination of temperature fields inside the PCM. These fields were determined from multiple temperature sensors and optionally in combination with a model-based estimation algorithm. Based on the known relation between temperature and phase fraction, phase fraction fields and mean phase fractions (SoC) in the PCM were calculated. Among many other studies applying temperature sensors within the PCM to monitor the phase change, one can mention Beaupere et al. [17], Charvat et al. [18], Zhou et al. [19], and Wang et al. [20]. Wang et al.

[20] used a relatively high number of temperature sensors to accurately measure the temperature distributions in the solid and the fluid domain in a small rectangular test cell. Barz et al. [21] evaluated a model-based sensor (soft-sensor) for the determination of characteristic temperature and phase fraction fields in the PCM in a lab-scale thermal energy storage with cylindrical PCM shells.

Energy flow sensors can, in principle, be applied for the determination of the SoC defined by the stored energy. These sensors could be used to measure the amount of heat supplied to and dissipated by the storage system, which could then allow determining the SoC via an energy balance. However, as previously stated, this method has the huge disadvantage of not being practicable as it requires very accurate and complex measurement technology as well as an accurate estimation of heat losses[9,22].

Image sensor or camera was also used for academic research to monitor phase front propagation in small test cells for studying specific phenomena and to derive from this the solid/liquid fraction of the PCM and the SoC. Charvat et al. [18] monitored the melting front propagation in a rectangular cavity filled with a paraffin-based PCM by means of a digital camera, although their study was not intended to monitor the SoC of the storage. An in-house image processing code was used for conversion of the photos into black and white images to monitor the propagation of the melting front and to assess the melt fraction. In another study, Klimes et al. [23,24] used the identified position of the melting front to assess the performance and accuracy of different simulation models based on the front tracking and interface capturing methods. Beaupere et al. [17] also used processed images from a camera to calculate solid fractions. Wang et al. [20] applied direct visual measurement of the liquid–solid interface in a small rectangular test cell to examine thermal characteristics of the melting process.

Level sensors can also be used to determine the solid/liquid phase front position and the SoC of a storage tank. Chazelle et al. [25] developed a system and method for determining the charge level of a reservoir partially filled with PCM, whose volume varied depending on the state of the PCM. Depending on the difference between the height of the fluid present in the reservoir when the PCM was completely discharged and charged, the SoC of the PCM could be determined. Henze et al. [26] used direct measurement of the ice level in a storage tank to estimate the SoC of a PCM storage.

Steinmaurer et al. [9] applied a method based on measurements of oscillating crystals to estimate the SoC of a PCM storage system. The method consisted of the application of an alternating voltage to electrodes made of quartz crystal and measurement of impedance, which depends on the phase state of the PCM. The main limitations of this method are that it is only applicable locally and the required impedance measurement has very high costs associated.

Propagation of sound was also investigated to determine the SoC of PCM storage systems. Steinmaurer et al. [9] performed global measurement of the propagation of structure-borne sound in the storage tank excitation by means of a pulse generator (e.g., electromagnet for striking) and measurement of the pressure fluctuation by means of piezoelectric acceleration sensors. The main advantages of this method are its relatively low costs, it is globally applicable, and it only requires one sensor to characterize the mean phase state. On the other hand, this method has the disadvantage of requiring complex calibration.

Waschull et al. [27] used electrical resistance measurement of conductive silicone membrane, which changes its electrical conductivity almost linearly depending on the mechanical stress, to generate the SoC signal. The storage tank was tightly sealed with such a silicone membrane, and volume variations of the PCM due to phase change produced different levels of membrane strain and the consequent variation of the electrical resistance. The disadvantages of this method are that it can only by applied for materials with a sufficiently high-volume change during phase change, as well as for designs with a very simple geometry.

Other methods for determination of the SoC of PCM storage systems, mainly used for academic research, consist of PCM viscosity measurement [8], impedance spectroscopy [8], neutron diffractometer [28], light transmission measurements [8,17], and/or reaction measurements[22].

From the literature review performed, it can be said that the technological maturity of available methods for determining the SoC of latent heat storage systems based on the use of water/ice as an

energy storage material is mature. Commercial sensors are available for this method [29]. For other different solid/liquid PCM, especially those in the industrially relevant temperature range of 80–300 °C, several patents were granted for techniques based on pressure sensors (no applications reported), electrical conductivity, temperature sensors, and a level sensor, all of these indicating a higher potential for practical application.

All measurement techniques can be grouped according to the following points:

1. The sensor applied to obtain a measurement signal, realizing either:
   1A. A local measurement for determination of a quantity at a specific position in the PCM or storage tank, or
   1B. A global or integral measurement for determining a mean or average quantity.
2. Aims at measurement of quantities which are sensitive to changes, either in:
   2A. The PCM state, being either solid or liquid, or
   2B. The energy of the PCM and/or storage system.

Group 2A techniques focus on the monitoring of changes in the PCM average phase fraction of solid/liquid PCM, while group 2B techniques focus on the monitoring of the amount of absorbed (or released) heat. Accordingly, both groups use a different definition of the SoC (also see Reference [21] for a discussion on that point). For group 2A, the following definition is used:

Definition 1: *The SoC indicates the extent to which a storage with PCM is charged relative to storable latent heat, i.e., the phase transition enthalpy of the PCM during melting and solidification.*

For group 2B, the following definition is used:

Definition 2: *The SoC indicates the extent to which a storage with PCM is charged relative to a maximal storable energy calculated from actual charging/discharging and reference temperatures.*

According to these points, the aforementioned most relevant measurement techniques are grouped as shown in Table 1.

Table 1. Classification of the most relevant measurement techniques for determination of the State of Charge (SoC).

Method	1A	1B	2A	2B
Electrical conductivity sensor	×		×	
Pressure sensor		×	×	
Temperature sensor		×		×
Energy flow sensor		×		×
Image processing from digital camera		×	×	
Level sensor		×	×	
Oscillating crystals	×		×	
Propagation of sound		×	×	
Propagation of ultrasonic	×		×	
Dielectricity, capacitance measurement	×		×	
Resistance measurement	×		×	
Light transmission measurements	×		×	

Various approaches exist to improve the performance of the aforementioned techniques. For instance, in order to provide global information of the PCM or thermal energy storage state, various local sensors can be used simultaneously, either to more accurately resolve thermodynamic states in the storage or PCM, or to more accurately track the evolution of the solid/liquid phase front. Examples are the combination of various local electrical conductivity or temperature sensors, and calculation of mean or average quantities [29]. However, this approach comes at the price of increased complexity and/or costs, making the method less attractive. It is limited in that the high resolution in possibly complex PCM geometries can easily require a prohibitively high number of sensors.

In addition, model-based algorithms can increase the accuracy of data obtained from sensors, e.g., to improve the accuracy of approximated temperature fields based on the solution of a heat transfer equation, or to improve the estimation of the mean PCM state using known PCM thermophysical relations to calculate PCM phase fractions from temperature data (e.g., Reference [21]).

Finally, the different techniques perform very differently for different PCM and storage internals and container geometries. Moreover, the compatibility of the sensors with relevant temperature ranges and materials needs to be evaluated. Finally, there is the question whether these sensors are established sensor technologies in the aimed use case, e.g., building or industrial applications.

The main objective of this paper is to study and assess four different methods for the determination of the SoC in a realistic experimental set-up and operating conditions, using established sensor technologies in industry as well as commercial industrial grade PCM integrated in a compact thermal energy storage with efficient and cost-effective heat exchanger (HEX) geometry for efficient charging and discharging operation. Different techniques are analyzed, which are based on pressure and temperature measurements for the determination of the SoC of a thermal energy storage tank filled with the commercial RT-4 [30] PCM.

The methods are based on local and global measurement techniques and are used to quantify the stored energy using the above-mentioned Definition 2 to define the SoC. Moreover, the issue of how to process signals from the pressure sensor to distinguish between variations due to volume changes in the PCM and to temperature variations in the range outside the phase change temperature range is discussed. Finally, advantages and disadvantages of the different measurement techniques and data processing methods are discussed and direction for future work are given.

2. Materials and Methods

The considered thermal energy storage system is part of a compact hybrid electric/thermal energy storage system, which is currently being developed for Mediterranean climates standalone or district connected residential buildings developed in the H2020 project, HYBUILD [31]. The TES tank is connected to a photovoltaic-driven (PV-driven) compression heat pump (HP), which is primarily used for space cooling. The TES is primarily used to store the cold produced by the HP during the periods of high availability of solar radiation and to cool the building when convenient from the energy and/or cost points of view. A key point in the development of an optimized control strategy is the continuous monitoring of the SoC of the TES tank. This parameter will be used as an input to decide whether to use energy from the PV panels, from the electrical or thermal energy storage, or electricity from the grid, to efficiently meet the energy requirements of the building.

2.1. Materials

The commercial RT-4 product provided by the company Rubitherm [30] was used as PCM in all experimental tests. It is an organic material, chemically inert, and thermally stable, therefore a constant behavior is expected for a large number of charges and discharges cycles. According to the data sheet provided by the manufacturer [30], it has a phase change temperature in the range between 2 and 4 °C, which suits the requirements of the specific application for which the PCM tank will be used. The relevant thermo-physical properties of RT-4 are shown in Table 2. **Error! Reference source not found.**a shows the partial specific enthalpy of the PCM according to its data sheet.

Table 2. Properties of the RT-4 commercial phase change materials (PCM) as given by the manufacturer [30].

Properties	Value	Units
Phase change range	2–4	°C
Density	0.88 (solid) 0.77 (liquid)	$kg \cdot L^{-1}$
Thermal conductivity	0.2	$W \cdot m^{-1} \cdot K^{-1}$

Volume expansion	12.5	%

Since the partial specific enthalpy of the PCM is a key input for the determination of the SoC of the PCM, experimental values were used in the present study. Experimental data were obtained by differential scanning calorimetry (DSC) analysis performed using the DSC 3+ Mettler Toledo equipment available at the GREiA research group at the University of Lleida (UdL). Heat flux measurements were obtained for different melting and solidification processes performed with a small sample of PCM within the temperature range between −18 and 28 °C at a constant heating/cooling rate of 0.5 K/minute. According to experimental data, the partial specific enthalpy of RT-4 is slightly different, as shown in **Error! Reference source not found.**b.

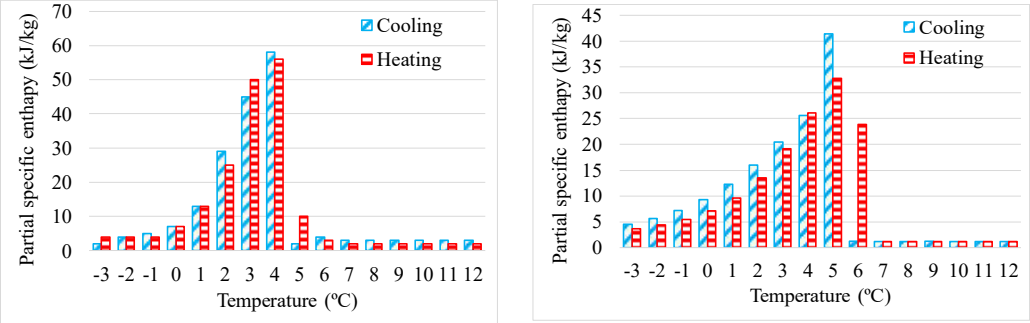

Figure 1. Partial specific enthalpy of RT-4. (**a**) Data taken from Reference [30], (**b**) DSC analysis by the authors.

A mixture of 70% water and 30% mono ethylene glycol was used as heat transfer fluid (HTF). Some of the relevant thermo-physical properties of the HTF are shown in Table 3, which were calculated by interpolating the values provided by the manufacturer at different temperatures [32].

Table 3. Properties of the heat transfer fluid (HTF) used, as given by the manufacturer [32].

Properties	At T = −2 °C	At T = 12 °C	Units
Density	1052.7	1047.4	$kg \cdot m^{-3}$
Viscosity	4.5	2.8	mPa·s
Specific heat	3585	3624	$J \cdot kg^{-1} \cdot K^{-1}$
Conductivity	0.421	0.437	$W \cdot m^{-1} \cdot K^{-1}$

2.2. Experimental Set-up

The experimental test rig shown in Figure 2 was built in the laboratory of the GREiA research group to perform different PCM charging and discharging processes in different configurations. It consists of two temperature-controlled water baths filled with the HTF, a HEX filled with 2.49 kg of RT-4 PCM connected to a DAB VA 65/180 wet rotor pump to recirculate the HTF through the HEX, a Badger Meter Primo Advanced flow meter, with an accuracy of ±0.25%, two three-way valves to switch the HTF flow between the hot or the cold HTF bath, 0.5″ copper pipes insulated with 18 × 0.9 mm polyurethane tubes, and valves. The cold and hot HTF baths had a capacity of 12 L and 20 L, respectively. Auxiliary units such as two JP SELECTA FRIGEDOR cooling coils, an OVAN TH100E immersion thermostat, and a JP SELECTA Termotronic immersion thermostat were used to control the temperature in both the cold and the hot HTF baths.

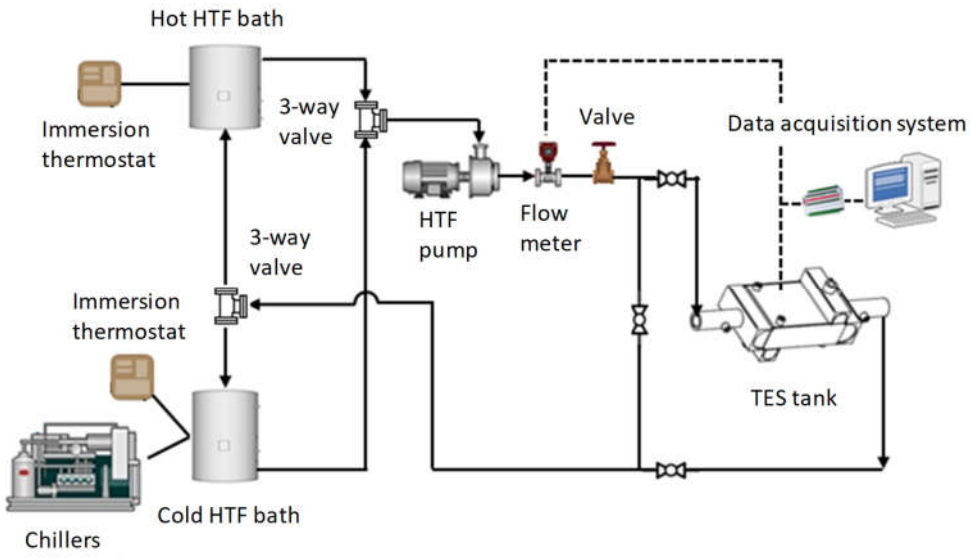

Figure 2. Schematic view of the experimental set-up.

The HEX design corresponds to the so-called compact heat exchanger design, which is widely applied for air conditioning and refrigeration systems [33]. It is an aluminum plate-fin extended surfaces heat exchanger with 14 parallel liquid passages of 3 mm height, and 15 air passages of 10 mm height. The core length (dimension of HEX internals) is 300 × 216 × 94 mm. The HTF flows through the liquid passages, while the air passages are filled with PCM and hermetically sealed.

The test rig and the HEX were equipped with different temperature sensors located at relevant positions and one pressure sensor. Seven Pt-100 class B temperature sensors with an accuracy of ±0.3 °C were used, five of them within the HEX to measure the PCM temperature at different locations, and two of them at the inlet and outlet of the HEX to measure the HTF temperature. Furthermore, an FG 10S20 WIKA pressure sensor with an accuracy ±0.25% was used to measure the pressure inside the HEX cavity where PCM was placed. The temperature in the HTF baths and the mass flow of the HTF were monitored as well. A data acquisition system consisting of a STEP DL-01 data logger connected to a personal computer was used to record the experimental measurements at a time interval of 30 s.

Figure 3 shows the details regarding the HEX configuration and the location of the temperature and pressure sensors within the heat exchanger. As shown in Figure 3a, the volume of the HEX filled with PCM has two cavities: an upper cavity that is filled with air and a lower cavity filled with PCM. The PCM was introduced through the upper opening until it reached the desired filling level, after which the pressure sensor was placed on the upper opening to hermetically close the PCM cavity. The details regarding HTF and PCM channels distribution are shown in Figure 3b, while the locations of the temperature and pressure sensors are shown in Figure 3c. Sensors T_1 and T_2, as well as T_4 and T_5 were placed symmetrically with respect to the horizontal plane that crosses the HEX through its center, while sensor T_3 was located in the center of the HEX.

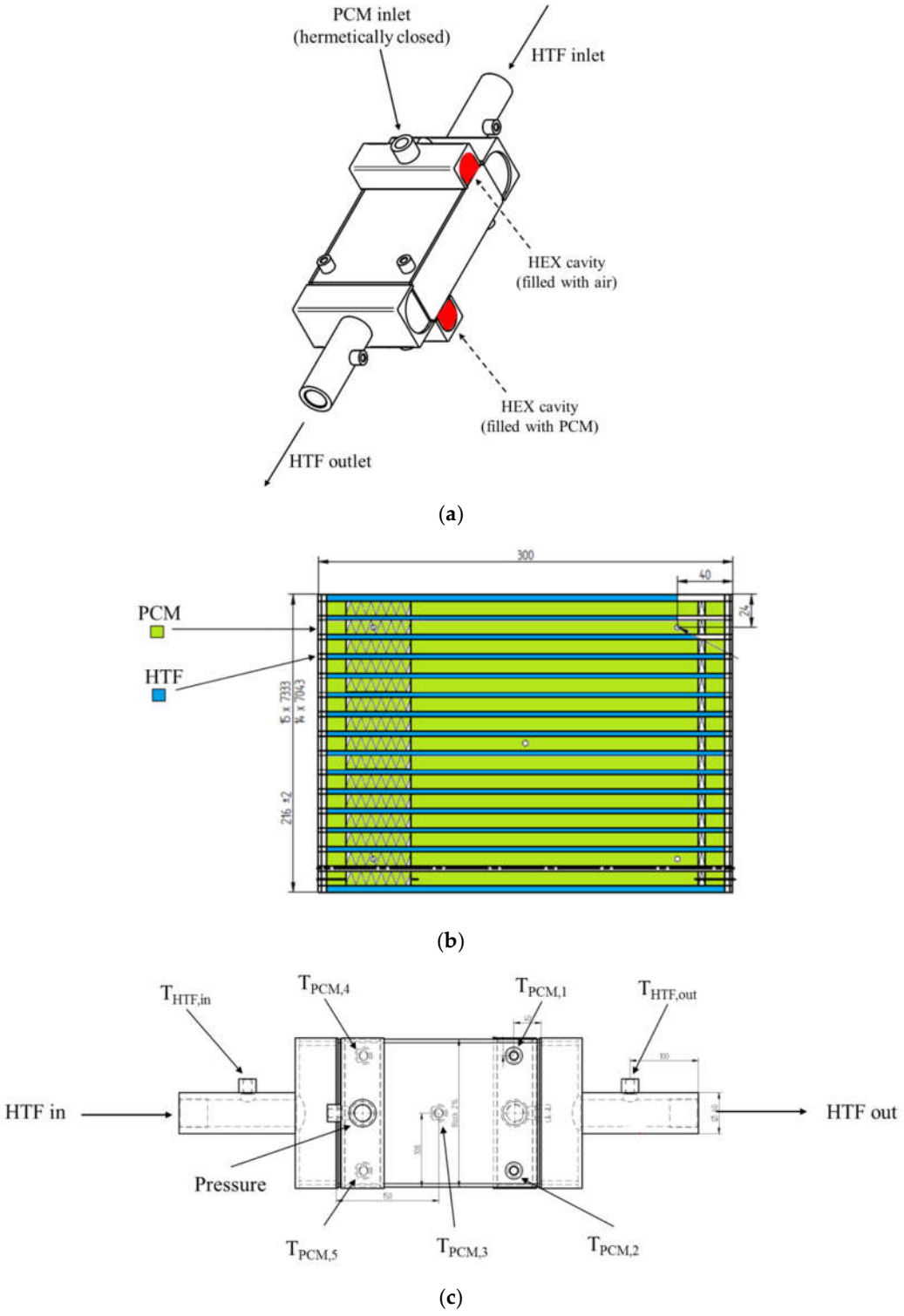

Figure 3. Heat exchanger (HEX) geometry: (**a**) three-dimensional (3D) view, (**b**) internal channels distribution, and (**c**) location of temperature and pressure sensors in the top view.

Figure 4 shows a picture of the experimental test rig, where the main components are indicated. The HEX is in the center of the figure covered by the insulating material.

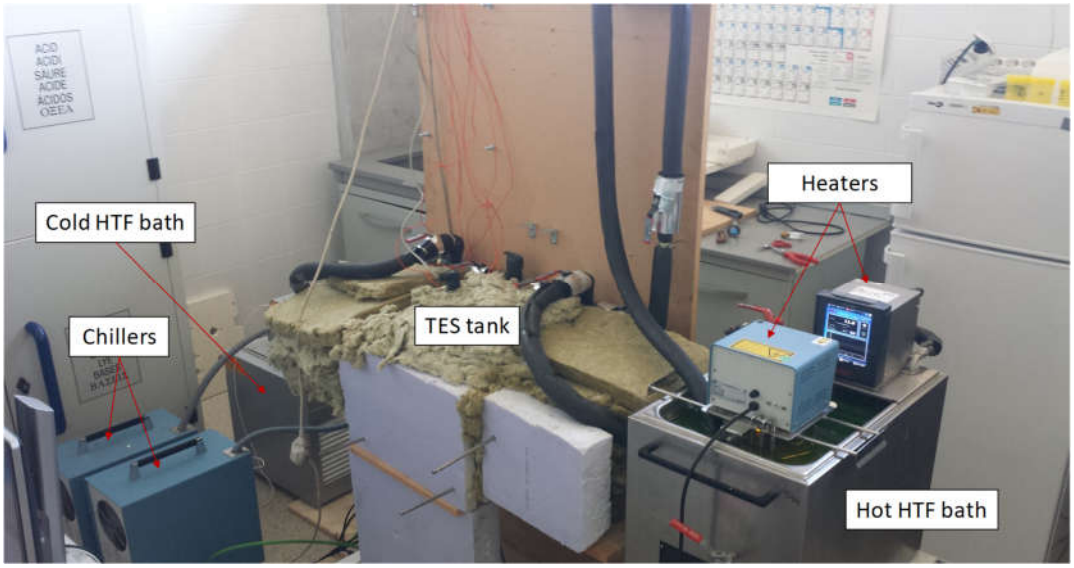

Figure 4. Photo of the experimental test rig.

2.3. Experimental Methodology

Several experiments were performed to evaluate alternative methods for the determination of the SoC under different operating conditions. Two operating scenarios were tested, as explained in Table 4. It should be noted that cooling applications are considered in this contribution. Thus, the TES tank is considered to be charged when the PCM is in the solid state.

The cold HTF bath was used as a source to charge cold within the TES tank through solidification of the PCM by supplying an inlet constant temperature to the HEX. The hot HTF bath was used to discharge the cold stored within the TES tank through melting of the PCM by supplying an inlet constant temperature to the HEX. The charging and discharging processes were considered completed when the average PCM temperature approached the HTF inlet temperature with a maximum deviation of 0.4 °C.

Table 4. Experimental design.

Charging experiment 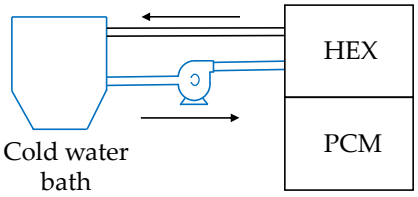 	For the charging process, the PCM was initially at a maximum temperature (T_{max}) that corresponds to a completely discharged state. Then, the two 3-way valves were switched to recirculate HTF from the cold tank through the HEX to charge the PCM with cold, until the TES tank got completely charged.
Discharging experiment 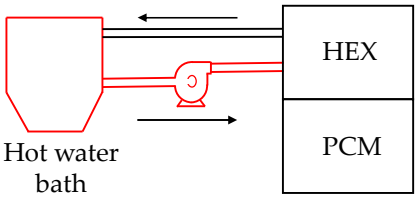 	For the discharging process, the PCM was initially at a minimum temperature (T_{min}) that corresponds to a completely charged state. Then, the two 3-way valves were switched to recirculate HTF from the hot tank through the HEX to discharge the cold from the PCM, until the TES tank got completely discharged.

Two types of experiments were performed, by varying the HTF flow rate for a fixed HTF inlet temperature and by varying the HTF inlet temperature for a fixed HTF flow rate (see Table 5 All

experiments were repeated three times to check the consistency in the results. Once all these tests were performed, the most representative experiment (i.e., the experiment with the most stable HEX inlet conditions) was selected to compare the different scenarios and to analyze the relation between flow, HTF inlet temperature, PCM temperatures, and the SoC.

Table 5. Experimental plan.

Type	Temperature range for the charging process (°C)	Temperature range for the discharging process (°C)	HTF flow rate (L/min)	Repetitions
Variable HTF flow rate	12 → −2	−2 → 12	2.0	3
	12 → −2	−2 → 12	1.5	3
	12 → −2	−2 → 12	1.0	3
	12 → −2	−2 → 12	0.5	3
Variable temperature range	14 → −3	−3 → 14	0.5	3
	12 → −2	−2 → 12	0.5	3
	10 → 1	1 →10	0.5	3

3. Theory and Calculations

Four different methods were used in this study to calculate the SoC of the TES tank, as described below. In each case, the TES tank was considered to be 100% charged when it reached the minimum level of energy, i.e., when it was able to provide then maximum amount of cold stored, while it was considered to be totally discharged when it reached the maximum level of energy.

3.1. Average PCM Temperature

The simplest way to estimate the SoC of the TES tank is based on calculating the average of the PCM temperature as shown in Equation (1). The main advantage of this method consists in the fact that the SoC can be obtained by means of a simple equation in terms of PCM temperature measurements. No detailed information is required regarding the PCM specific heat capacity and the SoC varies linearly with the PCM average temperature from 0 to 1. The SoC according to the average PCM temperature ($SoC_{T,PCM}$) is calculated using Equation (1):

$$SoC_{T,PCM} = \frac{T_{max} - \frac{\sum_i T_i(t) \cdot m_i}{M_{PCM}}}{T_{max} - T_{min}} \quad (1)$$

where $T_i(t)$ is the temperature of the PCM compartment i at time instant t, T_{min} and T_{max} are the minimum and maximum PCM temperature along the entire process respectively, m_i is the mass of the PCM associated to the PCM compartment i, and M_{PCM} is the total mass of PCM inside the HEX.

3.2. Average Specific PCM Enthalpy

In order to improve the previous method, the relation between PCM temperature and partial specific enthalpy (**Error! Reference source not found.**) was taken into account. In doing so, temperature is related to the amount of energy stored within the PCM. The SoC according to the average specific PCM ($SoC_{h,PCM}$) is calculated using Equation (2):

$$SoC_{h,PCM} = \frac{h_{max} - \frac{\sum_i h_i(t) \cdot m_i}{M_{PCM}}}{h_{max} - h_{min}} \quad (2)$$

where $h_i(t)$ is the specific enthalpy of the PCM compartment i at temperature T_i at time instant t, with h_{min} and h_{max} being the specific PCM enthalpy corresponding to T_{min} and T_{max}, respectively.

3.3. Energy Balance of the HTF

The temperature variation of the HTF as it flows through the HEX is the only source of energy that is being transferred to the TES tank, and the energy associated to this temperature variation can be considered as the maximum amount of energy that the PCM may store. However, this amount of energy is not only transferred to the PCM, but also to the aluminum casing of the HEX, the HTF that is inside the HEX, and also to the ambient as thermal losses. Therefore, in terms of absolute energy, the value obtained by means of an energy balance of the HTF will be different from the one obtained by applying the average enthalpy of the PCM method.

Nevertheless, the fact the SoC parameter is defined as a relative quantity allows to compare the different methods at any instant during the charging or discharging processes. Even so, the main drawback of this method consists in the fact that due to thermal losses, the amount of energy that can be restored from the TES tank will always be less than the maximum energy that is obtained by applying an energy balance of the HEX. If there is a large period between the charging and the discharging processes, heat losses during this period may be significant, and the SoC may give a wrong indication of the actual amount of cold that can be recovered from the TES tank.

The SoC is obtained in terms of the heat extracted from or supplied to the HEX by the HTF, depending on whether the TES tank is charging or discharging. The SoC according to the energy balance of the HTF (SOC_{HTF}) is calculated using Equation (3):

$$SOC_{HTF} = \begin{cases} \dfrac{\int_0^t \left(T_{HTF,out}(\tau) - T_{HTF,in}(\tau)\right) \cdot \mathrm{d}\tau}{\int_0^{t_f} \left(T_{HTF,out}(\tau) - T_{HTF,in}(\tau)\right) \cdot \mathrm{d}\tau}, \text{for charging} \\ 1 - \dfrac{\int_0^t \left(T_{HTF,in}(\tau) - T_{HTF,out}(\tau)\right) \cdot \mathrm{d}\tau}{\int_0^{t_f} \left(T_{HTF,in}(\tau) - T_{HTF,out}(\tau)\right) \cdot \mathrm{d}\tau}, \text{for discharging} \end{cases} \quad (3)$$

where $T_{HTF,in}$ and $T_{HTF,out}$ are the HTF temperature at the inlet and outlet of the HEX respectively, and t_f is the total duration of the charging/discharging process.

3.4. Pressure inside the PCM Cavity

The pressure inside the PCM cavity can vary because of two main effects: (1) variation of the PCM volume when it changes phase from liquid to solid states (and vice-versa) due to different values of the density in each state, and (2) temperature variation of the air trapped inside the PCM cavity, which causes an expansion or contraction of the air depending on whether the temperature increases or decreases, respectively. In this case, the two contributions have the same effect, that is, when the temperature increases above the PCM melting point, both the PCM and the air increase their volumes, so that the total pressure increase is the sum of both contributions. The opposite happens when the temperature decreases below the solidification point.

This method is based on the fact that the pressure inside the PCM cavity is expected to decrease when the PCM is solidifying because of its lower specific volume (higher density) in solid state, which allows the air trapped inside the PCM cavity to expand and decrease its pressure. Therefore, the minimum value of the pressure should indicate that the PCM is completely solidified, i.e., the TES tank is completely charged with cold. The SoC according to the pressure measured inside the PCM cavity (SOC_p) is calculated using Equation (4):

$$SOC_p = \frac{p_{max} - p(t)}{p_{max} - p_{min}} \quad (4)$$

where $p(t)$ is the pressure inside the PCM cavity at time instant t, and p_{min} and p_{max} are the minimum and the maximum pressure corresponding to T_{min} and T_{max}, respectively.

4. Results

4.1. Repeatability Tests

All the experimental tests shown in Table 5 were performed three times to ensure data reliability. Figure 5 shows the HTF inlet (T_{in}) and outlet (T_{out}) temperature evolution of three experiments for PCM charging (a) and discharging (b) processes for a HTF flow rate of 1.0 L/min. The results show that the temperature evolution is similar among the different experiments.

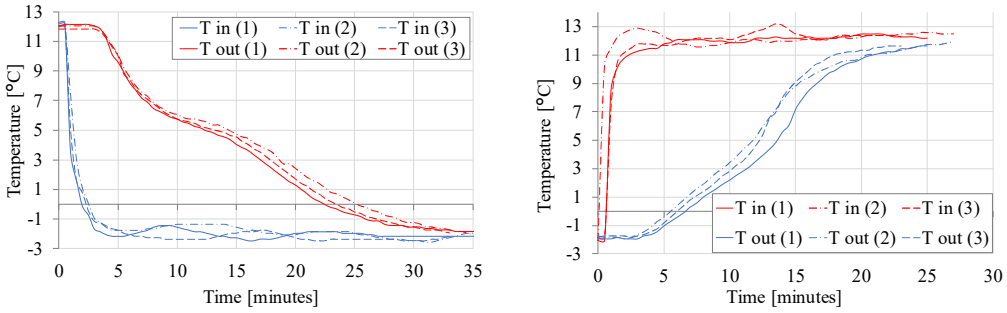

Figure 5. Results of HTF inlet and outlet temperature at a flow of 1 L/min for (**a**) charging and (**b**) discharging of PCM.

Figure 6 shows PCM temperature evolution of three experiments for PCM charging (a) and discharging (b) processes for a HTF flow rate of 1.0 L/min. Since the pair of temperature sensors positioned at the same distance inside the HEX along the direction of HTF flow (i.e., T_1 and T_2, and T_4 and T_5) had very similar values in all the experiments performed, the data of only one sensor of each pair is shown in all figures for simplicity. Here again, the temperature evolution is similar among the different experiments.

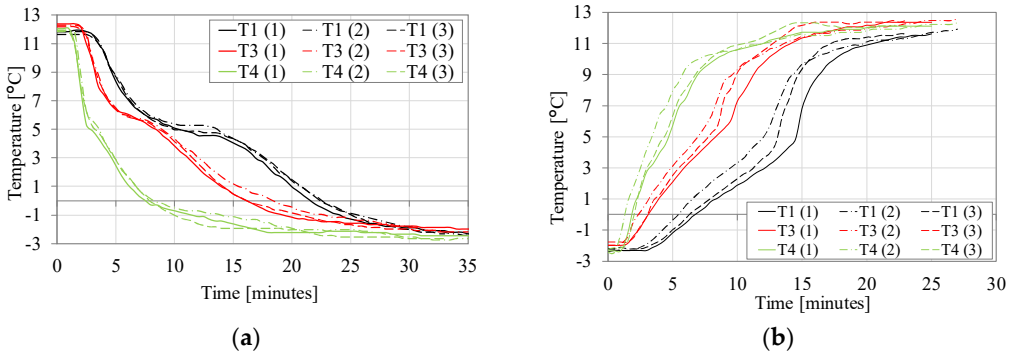

Figure 6. Results of repeatability of PCM temperature at a flow rate of 1 L/min for (**a**) charging and (**b**) discharging of PCM.

4.2. Evolution of PCM Temperatures during Charging and Discharging

Figure 7a shows the evolution of the PCM temperature at the relevant locations during charging at different HTF flow rates and constant HTF inlet temperature of −2 °C. The sensors located at a position closer to the inlet of the HEX (T_4) show an earlier and quicker temperature drop from the initial value of around 12 °C towards the final value around −2 °C for all flow rates. The effect of the PCM solidification, i.e., slowly changing temperatures within the phase transition temperature range especially around the peak of the PCM partial specific enthalpies in Figure 1b, can hardly be noticed at this location. However, for the sensor located in the middle of the HEX (T_3), this effect can be clearly seen when the temperature reaches about 6 °C. Here, the slope of the temperature drop is reduced

during a short time (approximately 1 min). This effect is more evident as the flow rate is lower (up to 6 min for 0.5 L/min). The sensors located closer to the outlet of the HEX (T_1) show a delayed and slower temperature drop, and the phase change effect is evident around 5 °C with an almost constant temperature for around 5 to 6 min. As expected, the overall duration of the charging process depends on the HTF flow rate, and it varies from about 17 min for a flow rate of 2 L/min to about 47 min for a flow rate of 0.5 L/min.

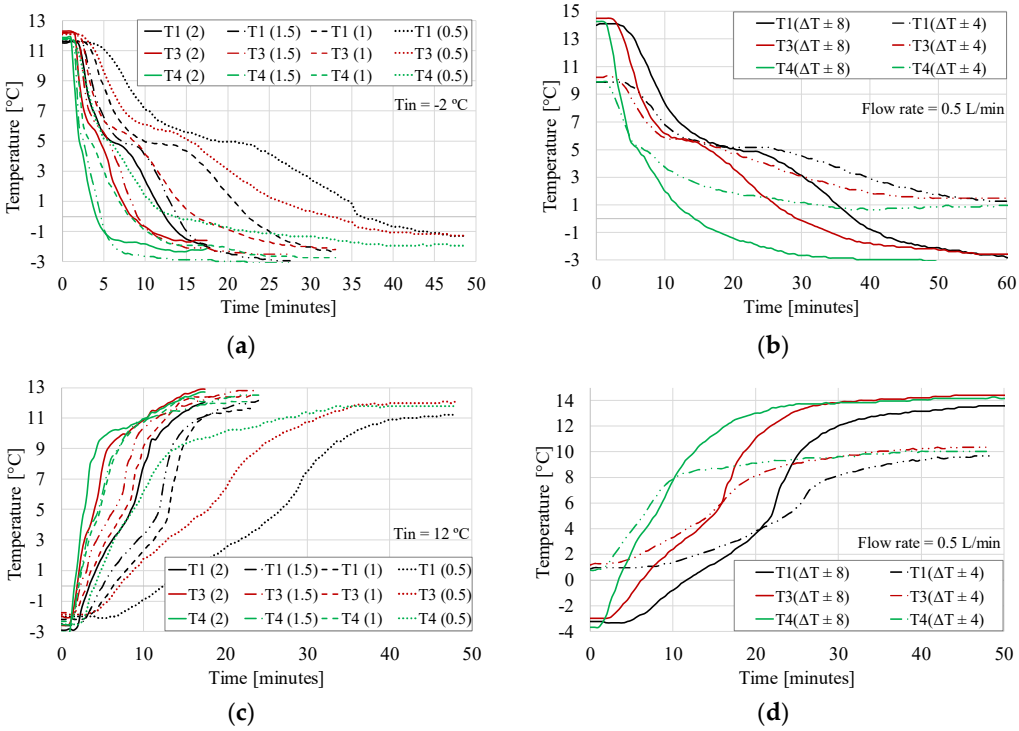

Figure 7. PCM temperature evolution at (**a**) different flow rates during the charging process, (**b**) different temperature ranges during the charging process, (**c**) different flow rates during the discharging process, and (**d**) different temperature ranges during the discharging process—Note that flow rate values (in L/min) and temperature ranges (K) are shown inside brackets in the legends. ΔT ±8 and ΔT ±4 in the legends of (b) and (d) refer to the temperature difference between the HTF inlet temperature and the peak of the PCM phase change temperature.

Figure 7b shows the temperature evolution of the PCM during charging processes for different temperature ranges and for a fixed flow rate of 0.5 L/min. The higher temperature range corresponds to a PCM temperature variation from 14 to −3 °C (denoted by ΔT ± 8 in the legend), while the lower temperature range corresponds to a PCM temperature variation from 10 to 1 °C (denoted by ΔT ± 4 in the legend).

Figure 7c shows the evolution of the PCM temperature during discharging at different HTF flow rates and constant HTF inlet temperature of 12 °C. Similar to the charging process, the change in temperature occurs faster for higher values of the HTF flow rate. The sensors located closer to the inlet of the HEX (T_4) show a faster change in temperature towards 12 °C. Unlike the charging process, the sensors located in the middle (T_3) and closer to the outlet of the HEX (T_1) do not show a significant reduction of the slope of temperature increase around the phase change temperature. This difference can be attributed to the different shape of the PCM specific heat capacity for solidification and melting (see Figure 1b).

Figure 7d shows the temperature evolution of the PCM during discharging processes for different temperature ranges and for a fixed flow rate of 0.5 L/min. The higher temperature range corresponds to a PCM temperature variation from −3 to 14 °C (denoted by ΔT ± 8 in the legend), while

the lower temperature range corresponds to a PCM temperature variation from 1 to 10 °C (denoted by ΔT ± 4 in the legend). The results are in line with results obtained in Figure 7b.

4.3. SoC—Average PCM Temperature Method

The SoC obtained by following this method is shown in Figure 8a for the charging process at different HTF flow rates and constant HTF inlet temperature of −2 °C. The SoC increases faster at the beginning of the process and it slows down its increase as the average PCM temperature approaches the inlet HTF temperature. The curves corresponding to the different HTF flow rates have similar features, although the time required to complete the process is lower for higher HTF flow rates, as expected.

The comparison of the SoC evolution for the charging process at a flow of 0.5 L/min for different temperature ranges is shown in Figure 8b. The two curves are almost identical, meaning that the temperature range has a very low influence on the evolution of the SoC with time during charging. There is a kink in the signal around 10 min, which might indicate that part of the PCM starts to solidify, as also observed in Figure 7b.

Results for discharging at different flow rates and constant HTF inlet temperature of 12 °C are shown in Figure 8c. Like in the charging process, the four curves show similar behavior, and the discharging is faster for higher HTF flow rates. The comparison of the SoC evolution for the discharging process at a flow of 0.5 L/min for different temperature ranges is shown in Figure 8d. In this case, it can be seen that the discharging process is slightly slower for the lower temperature range ΔT ± 4 °C, especially after 10 min from the beginning of the process. Again, as in Figure 7b and Figure 7d the shape of the curve for charging and discharging is different (e.g., in Figure 8d there is no kink around 10 min while there is a kink in Figure 8b), and can be attributed to the different shape of the PCM specific heat capacity for solidification and melting.

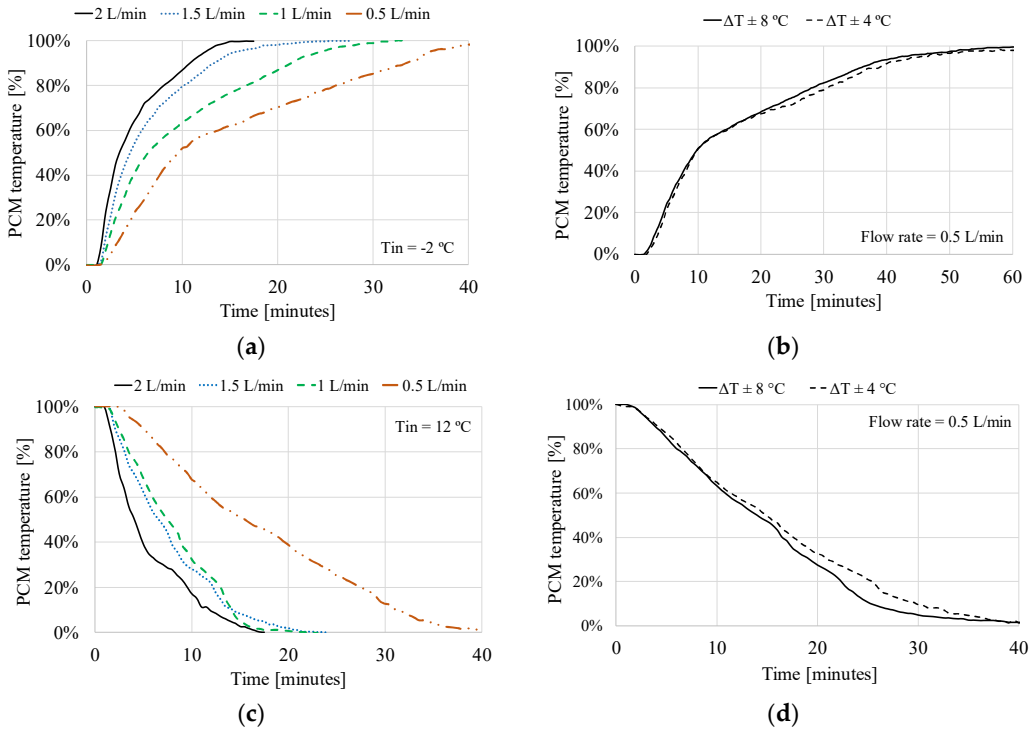

Figure 8. SoC according to PCM average temperature method at (**a**) different flow rates for the charging process, (**b**) different temperature ranges for the charging process, (**c**) different flow rates for the discharging process, and (**d**) different temperature ranges for the discharging process.

4.4. SoC—Average PCM Enthalpy Method

The SoC calculated according to the average PCM enthalpy method is shown in Figure 9a for the charging process at different flow rates and constant HTF inlet temperature of −2 °C. In all cases, the SoC starts to increase 1 min after the beginning of the charging process at a relatively high rate until it reaches around 80%, when the slope of the curve starts to decrease towards zero as the SoC approaches 100%. The slope of the SoC curve is higher for higher values of the HTF flow rate. The reason is that energy is transferred to the PCM at a higher rate at the beginning of the process because there is more temperature difference between the PCM and the HTF. For instance, at a flow rate of 1.5 L/min, a SoC value of 80% is reached in the first 10 min, while more than 20 min are needed to charge the rest of 20% required to reach a complete charge. This relation between SoC and time is similar for the different flow rates.

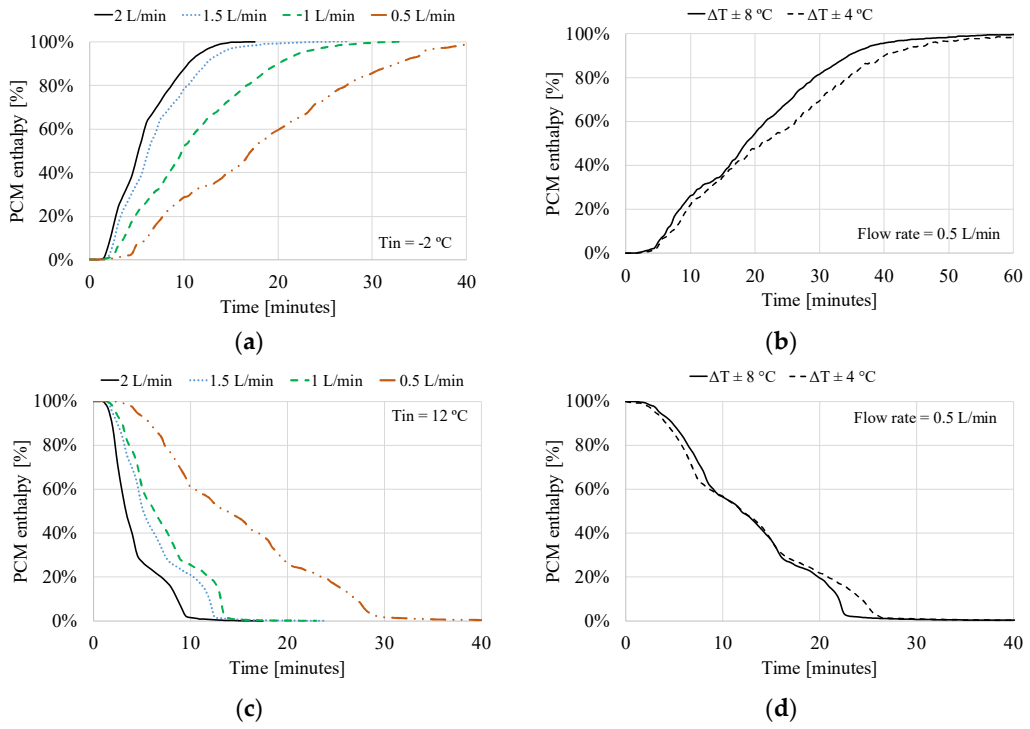

Figure 9. SoC according to the PCM average enthalpy method at (**a**) different flow rates for the charging process, (**b**) different temperature ranges for the charging process, (**c**) different flow rates for the discharging process, and (**d**) different temperature ranges for the discharging process.

The evolution of the SoC during the charging process at a flow of 0.5 L/min for different temperature ranges is shown in Figure 9b. The two curves are very similar during the first 15 min, after which the charging at a lower temperature range becomes slower than the other one.

The SoC evolution during the discharging process at different flow rates and constant HTF inlet temperature of 12 °C is shown in Figure 9c. When compared to the charging process, it can be noticed that the discharging process occurs faster and it is qualitatively different. Moreover, the slope of the predicted SoC curve for the discharging process shows strong variations that occur when the SoC is around 30%. This behavior is directly related to the evolution of the single PCM temperature measurements (and their average values) used to calculate the enthalpy values. In Figure 7c, it can be seen that for all flow rates, the temperature profiles show an inflection point at about 5–6 °C, which corresponds to the point where the melting of the PCM is completed and the temperatures start rising faster.

The comparison between the variations of the SoC for the discharging process at a flow of 0.5 L/min for different temperature ranges is shown in Figure 9d. The two curves are quite similar along the entire process, although the discharging at a lower temperature range (ΔT ± 4 °C) is initially slightly faster, and it finally becomes slower in the final part of the process. Again, as for Figure 9c,

the predicted SoC shows inflection points here for 35% and 60%, which might be caused by the sudden changes of the PCM specific partial enthalpies (Figure 1b) at the start and end of the melting process (see also the inflection points in Figure 7d). Finally, it can also be noticed that for the calculated SoC, the entire discharging process is faster than the corresponding charging for both temperature ranges.

4.5. SoC—Energy Balance of the HTF Method

The SoC calculated according to the HTF energy balance method is shown in Figure 10a for the charging process at different flow rates and constant HTF inlet temperature of −2 °C. The SoC increases faster at the beginning of the process because of the larger temperature difference between the PCM and the HTF, and the rate of increase gradually diminishes until the TES tank is completely charged. As already seen in previous figures, the charging process occurs faster at higher HTF flow rates. The evolution of the SoC for charging process at a flow of 0.5 L/min for different temperature ranges is shown in Figure 10b. The two curves are similar, and only a slight difference can be noticed at the middle part of the process, which does not affect that overall process duration that is practically the same in both cases.

The SoC evolution for discharging at different flow rates and constant HTF inlet temperature of 12 °C is shown in Figure 10c. The curves behave as expected, i.e., the SoC decreases faster at the beginning of the process and the process occurs faster at higher HTF flow rates. The evolution of the SoC for the discharging process at a flow of 0.5 L/min for different temperature ranges is shown in Figure 10d. In this case, again, the temperature range has practically no influence on the SoC time evolution, which are very similar for both values of the temperature range.

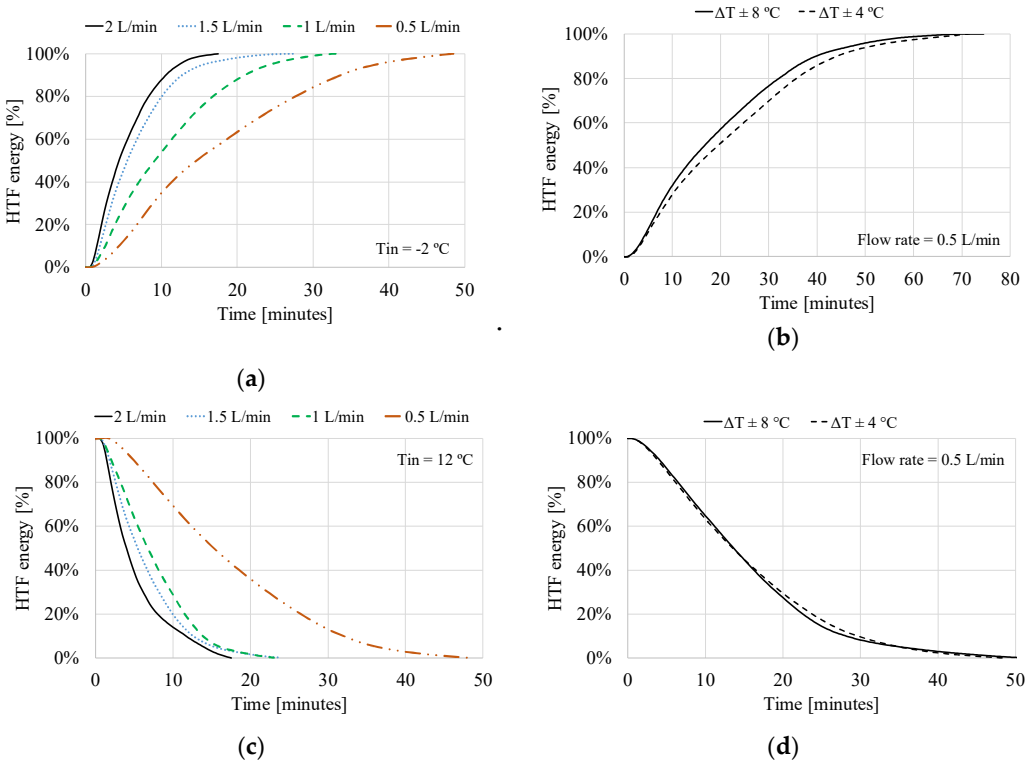

Figure 10. SoC according to the HTF energy balance method at (**a**) different flow rates for the charging process, (**b**) different temperature ranges for the charging process, (**c**) different flow rates for the discharging process, and (**d**) different temperature ranges for the discharging process.

4.6. SoC—Pressure inside the PCM Cavity Method

Figure 11a shows the SoC evolution according to the pressure method for the charging process at different flow rates and constant HTF inlet temperature of −2 °C. The SoC rate of increase is faster in the first half of the charging process, after which it slows down until the TES tank is completely charged. For instance, at a flow rate of 1.5 L/min, it can be noticed how after the first 4 min, the SoC already reaches a value of 50%, while it takes more than 10 min to charge the rest of the 50% needed to reach complete charging. This can be explained by the fact that the heat transfer rate is higher at the beginning of the process because of a larger temperature difference between the HTF and the PCM, which causes a faster temperature variation of both the PCM and the air inside the PCM cavity. The maximum slope of the predicted SoC curve is attained when the average PCM temperature is close to the phase change point, when the volumetric change of the PCM is more pronounced. The overall evolution of pressure is quite similar among the different flow rates, the pressure increase being higher for higher values of the HTF flow rate.

The evolution of the SoC for the charging process at a flow of 0.5 L/min for different temperature ranges is shown in Figure 11b. The SoC increases faster for a higher temperature range (ΔT ± 8 °C) during the first part of the process, and it slows down its increase in the second half of the process. As a consequence, a maximum SoC difference of around 20% between the two curves is achieved in the central part of the process.

The SoC evolution according to the PCM cavity pressure method during discharging at different flow rates and constant HTF inlet temperature of 12 °C is shown in Figure 11c. The evolution of pressure is generally quite similar among the different curves, the SoC decrease being faster at higher values of the HTF flow rate. As in the charging case, the pressure variations are faster at the beginning of the process, considerably decreasing towards the end of the process when the PCM is almost discharged. The evolution of the SoC during the discharging process at a flow of 0.5 L/min for different temperature ranges is shown in Figure 11d. Similar to the charging process, the SoC varies faster for a higher temperature range (ΔT ±8 °C) during the first part of the process, which produces a maximum SoC difference of more than 15% between the two curves after the first 7 min.

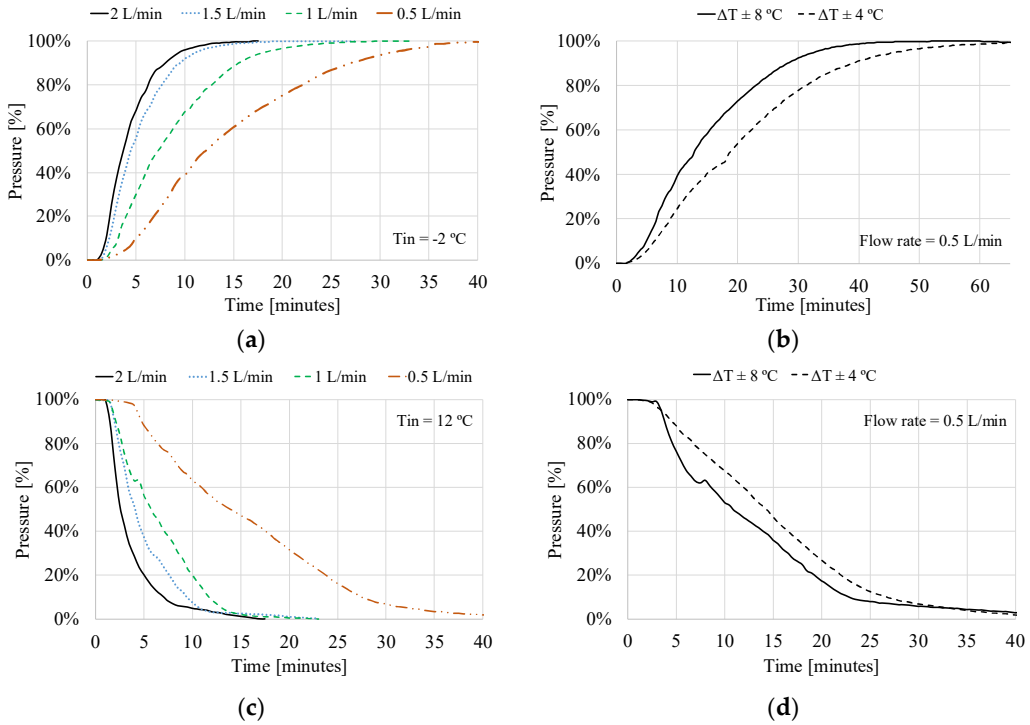

Figure 11. SoC according to the PCM cavity pressure method at (**a**) different flow rates for the charging process, (**b**) different temperature ranges for the charging process, (**c**) different flow rates for the discharging process, and (**d**) different temperature ranges for the discharging process.

4.7. Comparison of the Four SoC Methods Studied

The four methods investigated in this study are summarized and compared in this section, for several charging and discharging processes performed in the temperature range between −2 and 12 °C, and at four different HTF flow rates. Figure 12 shows that, during charging, a consistent relationship exists between the methods based on PCM enthalpy estimation and energy balance of the HTF, which follow similar trends along most of the process duration for each of the flow rates. However, the method based on PCM average temperature measurements predicts a faster increase at the first part of the process, and when the SoC reaches a value around 50%, there is a clear reduction in the rate of increase, and it adjusts to the previous two curves when the SoC is around 80%. Finally, the method based on pressure measurements also shows a different behavior with respect to the other three methods. At the beginning of the process, it increases at similar rates as the other methods, but unlike the other curves, in this case, the increase is maintained at a similar level as at the beginning until it reaches values almost as high as 90%.

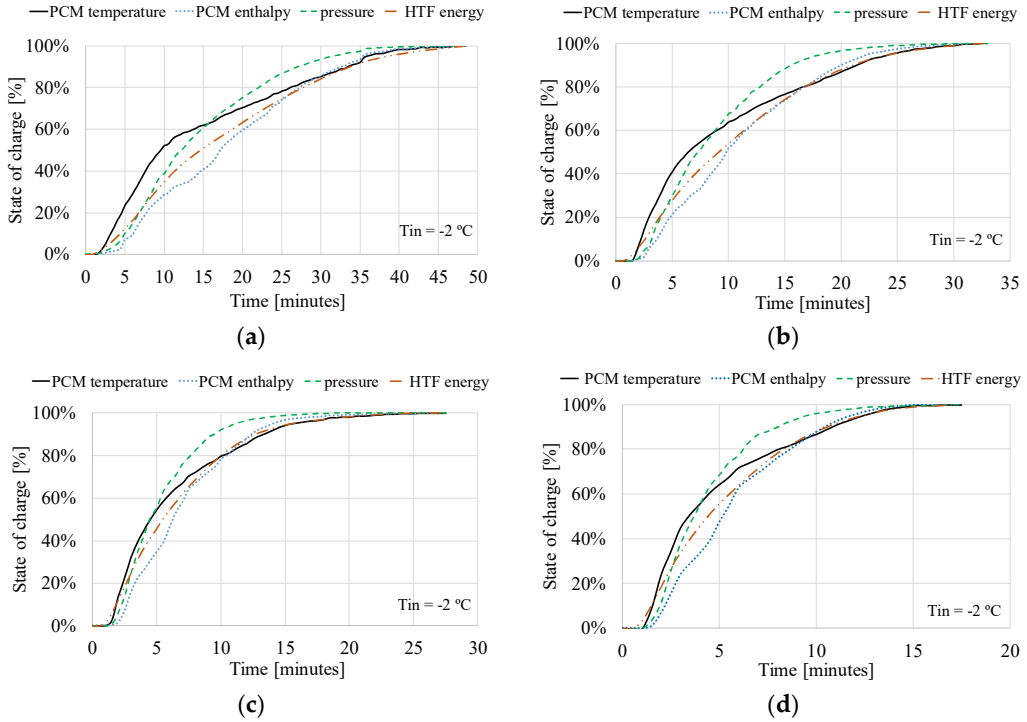

Figure 12. Comparison between the four methods for determining the SoC during charging at a HTF flow rate of (**a**) 0.5 L/min, (**b**) 1.0 L/min, (**c**) 1.5 L/min, and (**d**) 2 L/min.

Very similar results are obtained for the charging process at a flow rate of 0.5 L/min and at different temperature ranges (not shown here).

The evolution of the SoC according to the different methods during discharging at different HTF flow rates is shown in Figure 13. Unlike the charging process, the methods based on PCM enthalpy and energy balance of the HTF give quite different curves during discharging. The curve based on HTF energy balance is decreasing smoothly towards its minimum value, while the curve based on PCM enthalpy shows large slope variations with inflection points along the entire process, especially for higher HTF flow rates (see also the discussion of this effect in Section 4.4). Like in the charging process, the curve based on pressure measurements has the highest variation rate during the first part of the process, therefore being the method that gives the lowest values for the SoC along the major part of the entire process. On the other hand, the curve based on the average PCM temperature has a different profile as compared to the charging profile, in this case, being more similar to the profile of the curve based on the HTF energy balance.

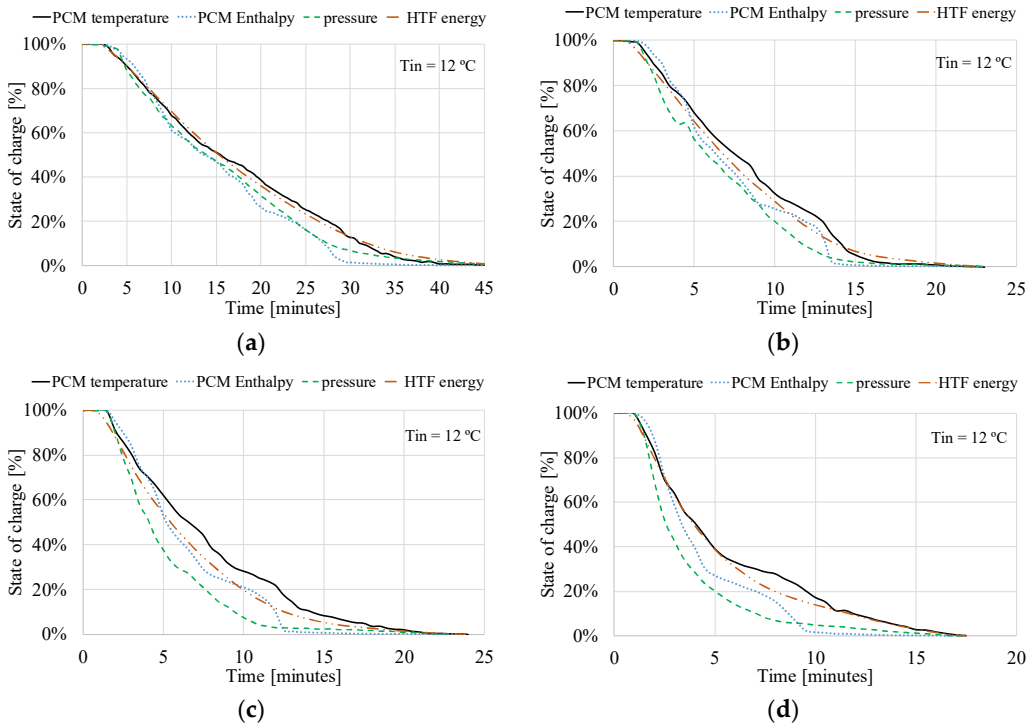

Figure 13. Comparison between the four methods for determining the SoC during discharging at a HTF flow rate of (**a**) 0.5 L/min, (**b**) 1.0 L/min, (**c**) 1.5 L/min, and (**d**) 2 L/min.

Very similar results are obtained for the discharging process at a flow rate of 0.5 L/min and at different temperature ranges (not shown here).

4.8. Detailed Analysis of the Pressure Signals inside and outside of the Phase Transition Temperature Range

An important aspect of the SoC method based on pressure measurements is to distinguish between the contributions coming from the sensible and latent temperature ranges. The sensible contribution is mainly due to the volume change of the air inside the cavity, and possibly from PCM expansion/contraction when it is totally liquid/solid. The latent contribution only comes from density variation of the PCM during phase change. Therefore, to quantify the magnitude of both sensible and latent contributions, an additional experiment was performed at a flow rate of 0.5 L/min in the sensible temperature range between 12 and 26 °C to compare it to a temperature range of the same amplitude between −2 and 12 °C, which includes the latent temperature range of the PCM.

Figure 14 shows the pressure variation in both sensible and latent temperature ranges. The temperature at the center of the HEX (T_3) is also shown in the graph to give a rough indication of the PCM SoC. During the first 40 min of the experiment, the PCM is cooled down in the sensible range from 26 to 12 °C. The pressure drop in this range is 0.17 bar, from 1.08 bar to 0.91 bar, due to the sensible contribution. During the next 40 min, the PCM is further cooled down from around 13 to −1 °C, and the pressure drops 0.36 bar, from 0.94 bar to 0.58 bar, due to both the sensible and latent contributions. Therefore, by subtracting the sensible contribution, one can get the latent contribution of 0.19 bar, which is almost the same as the sensible contribution. At around 120 min, the discharging process is initiated. The PCM is heated from −2 to 12 °C during 40 min, and the pressure increases 0.37 bar in this temperature range, from 0.59 bar to 0.96 bar. Finally, the PCM is heated in the sensible range from 13 to 26 °C, and the pressure increases 0.11 bar, from 0.97 to 1.08 bar. Thus, the pressure variation in the latent range is very similar for charging and discharging processes (0.36 bar versus 0.37 bar), while there is a slight difference in the sensible range, the variation during discharging being less than during charging (0.11 bar versus 0.19 bar). This may happen because the discharging process started immediately after the end of the charging, and the temperature distribution inside

the HEX may probably not be uniform, which can cause a deviation of the pressure inside the air cavity with respect to the expected value.

Figure 14 also shows an estimation of the latent contribution to the total pressure (denoted as 'Pressure_lat') that was obtained by subtracting the sensible contribution term, which was assumed to be a linear function of T3, from the total pressure. It can be noticed how the latent contribution is kept constant around 0.75 bar outside the phase change range, and it decreases to a minimum around 0.58 bar when the TES tank is supposed to be completely charged (no contribution from the sensible term). A slight deviation from the expected value of around 0.75 bar occurs just after the discharging process, where the latent term contribution increases to around 0.80 bar during 30 min, after which it slightly decreases towards 0.75 bar.

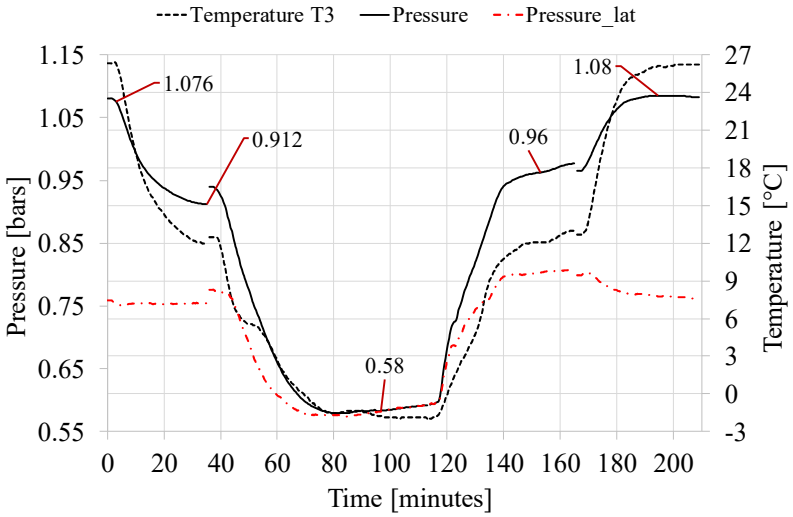

Figure 14. Pressure and temperature evolution in the sensible and latent temperature ranges for both charging and discharging processes at 0.5 L/min.

In view of the above analysis, the method based on pressure measurements inside the PCM cavity can be applied to estimate the SoC of the TES tank because there is a direct relation between the pressure and the state of the PCM. However, because of some effects that are related to the dynamics of successive charging or discharging processes, as well as particularities related to the specific configuration of the HEX studied here, some deviations from the typical and expected behavior may occur, which may affect the accuracy of the SoC obtained by means of this method.

5. Discussion

In this study, four different methods for the determination of the SoC of a small prototype of a TES tank filled with the commercial PCM RT4 for cooling applications in residential buildings were investigated, based on: (1) average PCM temperature, (2) average specific PCM enthalpy, (3) energy balance of the HTF, and (4) pressure inside the PCM cavity. All methods aim at the determination of the energy content of the PCM (according to Definition 2). The results show that for the considered application and instrumentation, each of these methods can be used to estimate the SoC.

Regarding the method based on average PCM temperature, it has the main advantage of being very simple and easy to implement. However, it assumes a linear relationship between temperature and SoC and thus, is not recommendable when an accurate estimation of the SoC is needed, e.g., during partial charging or discharging. The method based on the average specific PCM enthalpy improves the previous method relating temperature to specific enthalpies based on information on the PCM thermo-physical properties, and by this relating temperature to the amount of energy stored within the PCM.

For both temperature-based methods, to achieve accurate results, a large number of sensors is required, along with reliable information regarding the PCM specific enthalpy curve. If too few temperature sensors are used, as in the case of this study, the SoC shows large oscillations, especially in the discharging process, which denotes deviations from the SoC obtained using the other three methods. Furthermore, the use of established temperature measurement technology offers a robust solution for most solid/liquid storage systems, but with strong limitations regarding the accuracy of the derived SoC, in particular when a small number of sensors are used, when the PCM has variable or unknown thermo-physical properties, or in the case of complex geometries.

The method based on temperature measurement techniques has the advantage of using cheap sensors and established temperature measurement technology. However, it also has some disadvantages, such as the fact that it only applies locally and therefore it is not suitable for complex designs of latent heat accumulators. It is also problematic when PCM show hysteresis effects: in this case, the conversion of temperatures into specific enthalpies (and phase states) is only possible with comparatively complex mathematical models and strongly limited accuracy. If there are changes in the thermo-physical properties of the PCM due to, for instance, degradation of the material, this directly affects the performance of the process. Moreover, insufficient sensitivity of the sensors can lead to large errors for PCM with a small phase change temperature range ($T < 3K$).

Similar to the methods based on temperature measurement techniques, the method based on the energy balance of the HTF has the advantage of not requiring any information on the PCM. Moreover, this method can, in principle, be very accurate if additional information on the latent heat thermal energy storage is provided, such as the exact amount and specific heat of the casing material, average temperature of the casing material, amount and temperature of HTF inside the tank, ambient temperature, global heat transfer coefficient, and heat transfer surface area. The last three parameters allow calculating the heat transfer rate between the latent heat thermal energy storage and the ambient air, which is a key variable that is needed if this method is applied. Therefore, the main disadvantages of this method are the need for accurate additional information on the system, it is time-dependent due to heat transfer from the ambient, and it also required additional calculations to subtract the sensible heat stored in the casing material and the HTF inside the tank from the total energy to get the energy stored in the PCM only. This method is therefore used in this contribution to provide a reference value of the SoC. However, it is not recommended for practical applications.

Finally, the method based on pressure measurements inside the PCM cavity has the advantages that it only requires one pressure sensor, it does not require any information on the PCM, and it directly relates to the overall SoC of the PCM, regardless of its temperature distribution and the phase transition behavior (e.g., hysteresis effects for melting and solidification). The main limitation of this method is that it is only applicable for PCM that significantly change their volume during phase change. In contrast to previous studies, where the pressure sensors are considered to provide information regarding changes in the PCM volume during phase transition, in this study, it was shown that the pressure signal can be divided into sensible contribution (contribution from the air) and latent contribution (PCM density changes in the phase transition temperature range). Thus, the pressure sensor can provide information on the stored energy according to Definition 2. It was also noted, that for the experiments conducted, in some cases, a strange and unexpected behavior was observed, which can reduce the accuracy and reliability of the method. The performance of this technique relies on the critical assumptions that the pressure is homogenous within the entire storage tank even for complex designs, and that the storage tank is absolutely tight over the entire service life. In the case that all the above-mentioned assumptions are fulfilled, this technique is a global measurement method that provides information on the average PCM (phase) state in the storage system, and it only requires one pressure sensor. Another disadvantage might be that pressure sensors are less robust in long-term operation because they need to be periodically re-calibrated.

6. Conclusions

The implementation of energy storage systems is deemed necessary in most of the new technologies based on the use of renewable energies aimed at mitigating the use of fossil fuels and

their associated CO_2 emissions. In particular, the use of thermal energy storage within solar thermal systems for space heating and/or cooling in residential buildings could be a key element for achieving a significant reduction of the overall energy consumption and an improvement of the overall system efficiency.

For thermal energy storage systems based on the use of PCM, the information regarding the SoC is very important from the control strategy point of view. Therefore, a reliable method is deemed necessary to accurately determine the SoC of the PCM at any time. For solid/liquid PCM, different methods for SoC determination were previously investigated. A classification of the measurement techniques and data processing methods is given, distinguishing between local and global/integral measurement techniques, and using sensors that are either sensitive to changes in the PCM phase state, being either solid or liquid, or the energy of the PCM and/or energy storage system. Two corresponding alternative definitions of the SoC were introduced.

All four methods for determining the SoC of the PCM tank investigated in this study have both advantages and disadvantages. A good strategy in practical applications could be to combine two or more of these methods and take profit of the advantages of each of the methods. For instance, one could use the method based on pressure measurements combined with the average temperature method, which would not require any information on the PCM properties or tank characteristics. The temperature measurements could be used to determine the SoC outside the PCM phase changes range, i.e., when the tank is completely charged or discharged, while the pressure measurements could be used during the phase change. The transition from one method to the other would be dictated by the point when temperature measurements indicate the starting or finishing of the phase change process. Temperature measurements could also be used to calibrate the pressure measurements before each of the phase change processes.

Author Contributions: Conceptualization, G.Z. and J.G.; methodology, G.Z., J.G, T.B., and J.E.; software, C.O.; formal analysis, C.O.; investigation, G.Z., C.O., and J.G.; data curation, L.F.C..; writing—original draft preparation, G.Z. and C.O.; writing—review and editing, T.B., J.E., and L.F.C.; supervision, L.F.C.; project administration, L.F.C.; funding acquisition, L.F.C. All authors have read and agreed to the published version of the manuscript.

Funding: This project has received funding from the European Union's Horizon 2020 research and innovation programme under grant agreement No 768824 (HYBUILD). This work was partially funded by the Ministerio de Ciencia, Innovación y Universidades de España (RTI2018-093849-B-C31 - MCIU/AEI/FEDER, UE). This work was partially funded by the Ministerio de Ciencia, Innovación y Universidades - Agencia Estatal de Investigación (AEI) (RED2018-102431-T). This work is partially supported by ICREA under the ICREA Academia programme. Jaume Gasia would like to thank the Departament d'Universitats, Recerca i Societat de la Informació de la Generalitat de Catalunya for his research fellowship (2018 FI_B2 00100). The authors at the University of Lleida would like to thank the Catalan Government for the quality accreditation given to their research group (GREiA 2017 SGR 1537).

Acknowledgments: GREiA is a certified agent TECNIO in the category of technology developers from the Government of Catalonia.

Conflicts of Interest: The authors declare no conflict of interest. The funders had no role in the design of the study; in the collection, analyses, or interpretation of data; in the writing of the manuscript, or in the decision to publish the results.

Appendix—Lessons Learnt Applying the Pressure inside the PCM Cavity Method

Although the evaluation of the SoC based on pressure measurements inside the PCM cavity seems to be a reliable method because the pressure directly depends on the state of the PCM, some irregularities were observed in a few experiments. FigureA1a shows the evolution of the pressure in two charging processes performed at a flow rate of 1 L/min. The process denoted by 'A' shows a typical behavior of the pressure evolution, for which the pressure decreases from an initial value of about 0.90 bar to a final value between 0.55 bar and 0.60 bar. On the other hand, the process denoted by 'B' shows a different behavior, i.e., the pressure decreases from the initial value of 0.96 bar until it reaches a value around 0.75 bar when it suddenly stops decreasing and stabilizes around 0.73 bar, despite that fact that the PCM temperature keeps decreasing until the TES tank gets completely charged. This strange behavior of pressure variation could be explained by the solidification of the PCM in the region between the air cavity, where the pressure sensor is located, and the space where the PCM is located between the HTF channels, which could block the expansion of air inside the cavity, in this way creating a local overpressure.

A strange behavior was also observed in a few discharging processes. Figure A1b hows the evolution of the pressure in two discharging processes performed at a flow rate of 1 L/min. The process denoted by 'A' shows a typical behavior of the pressure evolution, for which the pressure increases from an initial value between 0.55 bar and 0.60 bar to a final value around 0.96 bar. In the case of the strange behavior denoted by 'B', the pressure starts at 0.75 bar, which is much higher than usual, and it increases until it reaches a value around 0.9 bar, after which it stops increasing and it even decreases for a short period, after which it recovers the normal evolution towards the maximum value of around 1.00 bar corresponding to complete discharging of the TES tank. The cause of such a strange behavior can be the same, or similar, as in the charging case. If initially the solid PCM blocks the space that allows communication between the air cavity and the space where the PCM is located, as the temperature of the air inside the cavity increases, the pressure also increases until the solid PCM that blocks the air cavity changes phase and finally allows the air trapped inside the cavity to redistribute inside the whole space where the PCM is located.

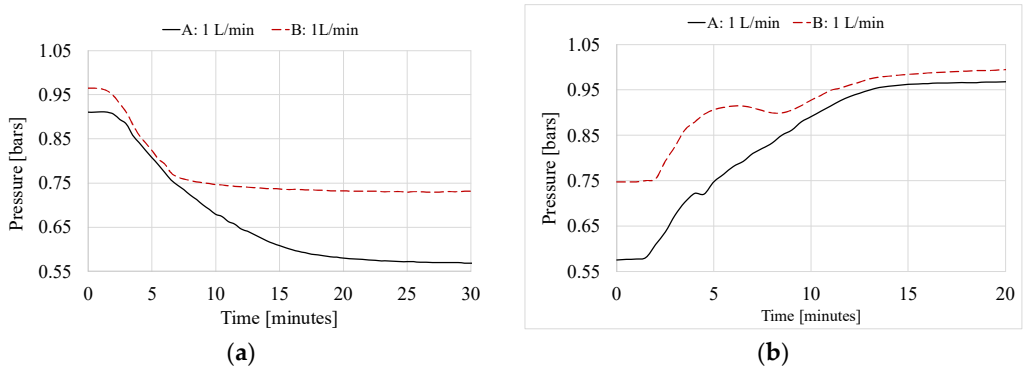

Figure A1. Examples of pressure evolution during (**a**) two charging processes at a flow rate of 1 L/min, and (**b**) two discharging processes at a flow rate of 1 L/min. Curve A shows the pressure behavior in most of the experiments, while curve B shows an unusual pressure behavior.

Another reason for the unusual pressure behavior could be related to air bubbles that may form during the solidification process, which may artificially increase the volume occupied by the PCM when it is completely solid. It is also possible that the PCM that occupies the second cavity of the HEX (see Figure 3) is in a state different from the state of the PCM that is in direct contact with the HTF channels if the duration of the charging and discharging processes, as well as the time period between two consecutive processes, is too short to allow the PCM to undergo a complete phase change.

To check this last hypothesis, the initial values of the pressure at the beginning of all charging and discharging processes performed were put together to compare the differences between the

experiments. Figure A2a shows the initial values of the pressure for charging processes with an initial temperature value around 12 °C and at different flow rates, while Figure A2b shows the initial values of the pressure for discharging processes with an initial temperature value around −2 °C and at different flow rates. Two types of experiments can be distinguished in both charging and discharging. The first one, denoted by 1st experiment, refers to experiments that were performed at the beginning of the day, so that the time lapse from the previous experiment performed the previous day is large enough for the system to have reached uniform and stable temperature distribution inside the HEX. The second one, denoted by 2nd experiment, are experiments that were performed the same day after a previous experiment, so that in this case the time lapse between the first and the second experiment is much shorter, and the HEX may not have reached a uniform temperature distribution. The strange pressure behavior occurred more frequently in the second experiment of the day, which could be a confirmation of the hypothesis that (part of) the PCM inside the cavity might remain solid/liquid from the previous charging/discharging process. Most of the second experiments start at a pressure that, in average, is 0.04 bars higher than the one of the 1st experiments of the day. Nevertheless, the strange behavior was also observed in a few of the first experiments, which indicates that there may be other reasons that may lead to such strange behavior.

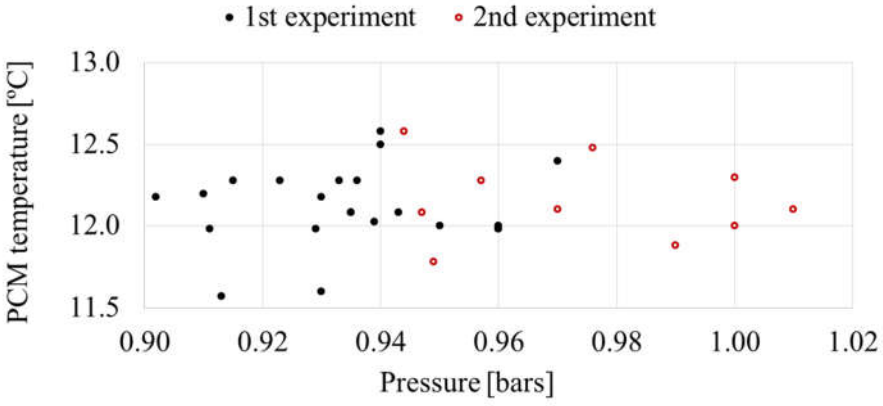

(**a**)

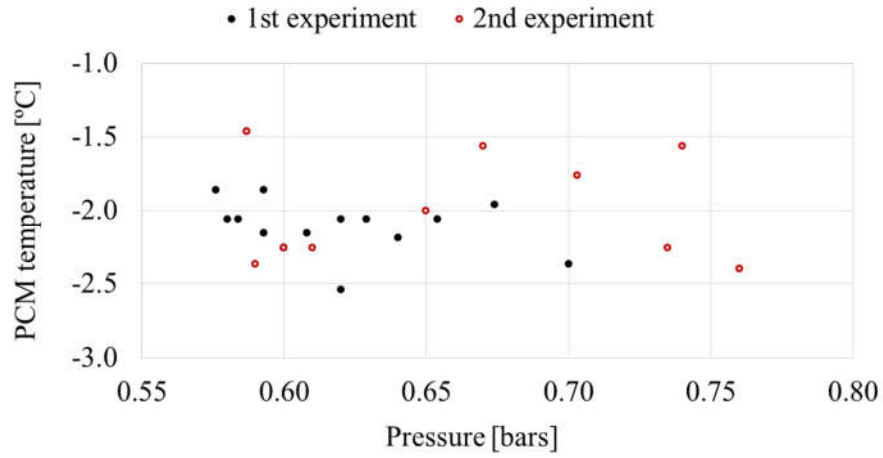

(**b**)

Figure A2. PCM temperature and pressure initial values before (**a**) charging and (**b**) discharging processes of daily experiments in the temperature range between −2 and 12 °C.

References

1. International Energy Agency. *Global Energy & CO2 Status Report 2017*; International Energy Agency: Paris,

France, 2018.
2. IEA-ETSAP and IRENA. *Solar Heating and Cooling for Residential Applications—Technology Brief*; IRENA: Abu Dhabi, UAE, 2015.
3. Cole, W.J.; Powell, K.M.; Edgar, T.F. Optimization and advanced control of thermal energy storage systems. *Rev. Chem. Eng.* **2012**, *28*, 81–99.
4. Powell, K.M.; Cole, W.J.; Ekarika, U.F.; Edgar, T.F. Optimal chiller loading in a district cooling system with thermal energy storage. *Energy* **2013**, *50*, 445–453.
5. Bauer, T.; Laing, D.; Steinmann, W.-D. Feasibility of the new PCM measurement system based on the electric resistance approach in lab scale demonstrated. In *Deliverable Report 15.4—Solar Facilities for the European Research Area (SFERA) Project*; 2012.
6. Bauer, T.; Steinmann, W.-D. Electrode Design for Latent Heat Storage; Patent DE102010001361A1, 8 April 2011.
7. Ezan, M.A.; Cetin, L.; Erek, A. Ice thickness measurement method for thermal energy storage unit. *J. Therm. Sci. Technol.* **2011**, *31*, 1–10.
8. Paberit, R.; Öjerborn, J. *Detecting State of Charge in PCMs—Experimental Investigation of Changes in Chemical and Physical Properties during Phase Transitions*; Chalmers University of Technology: Gothenburg, Sweden, 2016.
9. Steinmaurer, G.; Krupa, M.; Kefer, P. Development of sensors for measuring the enthalpy of PCM storage systems. *Energy Procedia* **2014**, *48*, 440–446.
10. Bissell, A.; Gataora, S.S. Heat Battery Assemblies and Monitoring System Therefor; Patent WO2014191778A1,4 December 2014.
11. Grama, S.; Dorson, M.H.; Christianson, R. *Thermal Energy Battery with Enhanced Heat Exchange Capability and Modularity*; Patent WO2014059163A1, 17 April 2014.
12. Dixler, K.; Kwok, W. Active and Passive Cooling for an Energy Storage Module; Patent US20140158340A1, 12 June 2014.
13. Ros, N. Insulation-Time Determining Device for a Thermally Insulated Container; Patent WO2015051474A1, 16 April 2015.
14. Viessmann Kaeltetechnik, A.G. Device for Determining the Charge State of a Segmented Thermal Storage; Patent DE202012103718U1, 3 January 2013.
15. Kazuhiro, D.; Tetsuya, I.; Yasuyuki, U.; Yuka, U.; Takashi, Y. Cooling Equipment, Temperature Control System, Air Conditioning System, and Hot Water Supply System for the Same; Patent US20140124158A1, 8 May 2014.
16. Barz, T. *Method for Determining the Charge Level of a Latent Heat Storage Device*; Patent EP3336473A1, 20 June 2018.
17. Beaupere, N.; Soupremanien, U.; Zalewski, L. Solidification monitoring of supercooled phase change materials. In *Proceedings of the 12th IIR Conference on Phase-Change Materials and Slurries for Refrigeration and Air Conditioning (PCM 2018)*; International Institute of Refrigeration (IIR): Orford, QC, Canada, 2018; pp. 166–173.
18. Charvát, P.; Štětina, J.; Mauder, T.; Klimeš, L. Visual monitoring of the melting front propagation in a paraffin-based PCM. *EPJ Web Conf.* **2017**, *143*, 02042.
19. Zhou, G.; Zhu, M.; Xiang, Y. Effect of percussion vibration on solidification of supercooled salt hydrate PCM in thermal storage unit. *Renew. Energy* **2018**, *126*, 537–544.
20. Wang, Y.; Amiri, A.; Vafai, K. An experimental investigation of the melting process in a rectangular enclosure. *Int. J. Heat Mass Transf.* **1999**, *42*, 3659–3672.
21. Barz, T.; Seliger, D.; Marx, K.; Sommer, A.; Walter, S.F.; Bock, H.G.; Körkel, S. State and state of charge estimation for a latent heat storage. *Control. Eng. Pract.* **2018**, *72*, 151–166.
22. Fischer, U.R.; Maschke, U.; Schneider, J. *Entwicklung Eines Messverfahrens zur Bestimmung des Thermischen Beladungsgrades von PCM-Paraffin-Speichern : Schlussbericht zum BMWi-Projekt 0327370F ; Verbundprojekt Energie Optimiertes Bauen (EnOB), Thematischer Verbund LowEx*; Brandenburg University of Technology: Cottbus, Germany, 2008.
23. Klimeš, L.; Mauder, T.; Charvát, P.; Štětina, J. A Front Tracking Method Accelerated by Graphics Processing Units for Phase Change Modelling in Latent Heat Thermal Energy Storage: A Comparison with Interface Capturing Methods. *Proc. Chem. Eng. Trans.* **2017**, *61, 1039-1044*.
24. Klimeš, L.; Mauder, T.; Charvát, P.; Štětina, J. Front tracking in modelling of latent heat thermal energy

storage: Assessment of accuracy and efficiency, benchmarking and GPU-based acceleration. *Energy* **2018**, *155*, 297–311.
25. Chazelle, B.; Couturier, R.; Martinelli, M. *System and Method for Determining the Charge Level of a Latent Heat Store*; Patent WO2016051377, 7 April 2016.
26. Henze, G.P.; Kalz, D.E.; Liu, S.; Felsmann, C. Experimental analysis of model-based predictive optimal control for active and passive building thermal storage inventory. *HVAC R Res.* **2005**, *11*, 189–213.
27. Waschull, J.; Müller, R.; Hernschier, W.; Künanz, R. Cold storage devices for smart grid integration. *Energy Procedia* **2014**, *46*, 48–57.
28. Sugo, H.; Kisi, E.; Bradley, J.; Fiedler, T.; Luzin, V. In situ neutron diffraction studies of operating MGA thermal storage materials. *Renew. Energy Environ. Sustain.* **2017**, *2*, 34.
29. Dincer, I.; Rosen, M.A. *Thermal Energy Storage: Systems and Applications*; Ltd, J.W.S., Ed.; Woodhead Publishing: Cambridge, UK, 2002.
30. Rubitherm. Available online: https://www.rubitherm.eu/en/index.php/productcategory/organische-pcm-rt (accessed on 15 January 2019).
31. Hybuild. Available online: http://www.hybuild.eu/ (accessed on 15 January 2019).
32. The Dow Chemical Company Dowtherm SR-1. Available online: https://corporate.dow.com (accessed on 25 June 2019).
33. Shah, R.K.; Sekulic, D.P. *Fundamentals of Heat Exchanger Design*; John Wiley & Sons: Hoboken, NJ, USA, 2003.